# PHASE PRESSURE MEASUREMENTS: SIMULTANEOUS AND DIRECT DERIVATION OF RELATIVE PERMEABILITY AND DYNAMIC CAPILLARY PRESSURE

**A.S. Lackner, Statoil ASA, and O. Torsaeter**
Norwegian University of Science and Technology

*This paper was prepared for presentation at the International Symposium of the Society of Core Analysts held in Toronto, Canada, 21-25 August 2005*

## ABSTRACT

A direct method for measuring dynamic phase pressures for water and oil and calculation of relative permeabilities is introduced. The method provides dynamic capillary pressure, which is necessary for a realistic calculation of relative permeabilities. By measuring the individual in-situ phase-pressures and saturation from material balance, the dynamic rock/fluid interaction properties were determined. Hence, the drawback of the traditional unsteady-state calculation method of relative permeability, namely neglecting capillary pressure is overcome.

Outcrop sandstone cores were confined in an epoxy sleeve, allowing small pressure-monitored water-and oil-wetting porous membranes to be in capillary contact with the rock fluids. Brine and Exxsol-D60 (dead oil) were used to represent oil and water and the experiments were performed at low pressure and temperature. Many prototype experiments testing different components were done. Eventually, drainage using different rates was performed followed by an imbibition process using a low capillary rate.

The combination of this method with in-situ saturation measurements and a traditional special core analysis method, gives an improved procedure for directly calculating relative permeabilities over the entire saturation range: For low and intermediate wetting phase saturations, where capillary forces are predominant, the new method is especially applicable. As the saturation increases, the traditional method will be sufficient for inverting the relative permeabilities. In future, this method can be applied to both unsteady- and steady-state commercial experiments, comprising both two- and three-phase processes.

## INTRODUCTION

When calculating relative permeabilities from experimental flow performance, capillarity is normally neglected by using high flooding rates [1]. The measured flow data are in practice history matched using a simulator [2], and the flow functions over the entire saturation range can be correctly retrieved. However, these data can be unrealistic because of the too high flow rate used in the experiments. Furthermore, due to experimental difficulties capillary pressure (Pc) is commonly measured in a static process using the centrifuge or porous plate technique [3, 4].

It is dubious that the dynamic capillarity present in a water-oil flooding process can be represented by statically measured capillary pressure [5]. Another drawback is that Pc is mostly measured on a different rock than used in the dynamic experiment, possibly supporting this experiment with the wrong set of data.

Richardson et al. [6] were the first to measure phase pressure in a flooding process. By using micro membranes, work was done to measure water and oil pressure at a fixed position in the core during flow [7] and in the literature a small number of similar publications exist on the problem of dynamic individual phase pressure measurements [8, 9, 10, 11, 12]. Assuming a travelling saturation wave propagating the porous media, Helset et al. [13] developed a theory for measuring relative permeabilities including capillarity for an unsteady-state process. Virnovsky and Skjæveland [14] proposed a laboratory procedure that uses multiple rates to correct for the capillary end effect in a steady-state process. A disadvantage of this procedure is that it is time consuming since each injection ratio of water and oil should be repeated at several different total rates.

Traditionally, relative permeabilities are calculated from experiments where pressure drop over the core ($\Delta P$) and the produced fluid volumes are measured outside the porous media. By accessing the individual phase pressures inside the rock, these functions, including their belonging dynamic Pc-curve can be acquired directly and realistically for any rate and constraint comparable to the conditions in a reservoir.

## MATERIAL AND METHOD

Sandstone core plugs were subject to prototype individual dynamic phase pressure measurements by coreflooding. After methanol cleaning and drying the cores, their size, mass and Helium porosity were measured. Table 1 shows the measured dry conventional core properties.

Table 1: Measured core conventional rock properties.

| Core | Transducer | L (cm) | A (cm2) | Vp (cm3) | K (mD) |
|---|---|---|---|---|---|
| P4-Bentheimer | RS | 13.45±0.05 | 11.3±0.1 | 37.0±1.8 | 950±20 |
| P7-Berea | MPX | 13.68±0.03 | 11.0±0.1 | 29±2 | 43±5 |
| P8-Berea | MPX | 13.6±0.1 | 27.9±1.7 | 27.9±1.7 | 47±2 |

Figure 1 shows the overall experimental setup. Also, a sketch of small pressure taps for both water, oil and, hence, Pc located at x/L=0.35-0.40 is shown. x denotes the distance from the core inlet to the pressure tap and L is the core length. The tap included a pressure transducer in contact with water- and oil-wet porous membranes, which were separated from the core surface by a pre-filter.

Small differential pressure transducers (MPX2200DP, Motorola, Inc. and RS 232-709, Honeywell International Inc.) with range 0-2 bar and with 5% full scale output error (FSO) were used. For a fast pressure response, the volume of the tap should, due to the effect of water compressibility and very low membrane permeability, be as small as possible.

We estimated this volume to 0.01±0.002 ml, which is much smaller than volumes reported in similar work [7], where a considerable tubing volume was used for communication between the transducer and the membrane. The pressure transducer ports were modified to fit the curved core surface before each transducer was calibrated against the ΔP (which is not equivalent to the capillary pressure) transducer (Fuji, Inc.). All pressures were continuously monitored and logged on a computer.

To find single phase wetting membranes that fitted our experimental constraints, several trademarks were evaluated and some were tested. Both the water- and oil-wet membrane, located between the transducer and the core side, should at least resist a non-wetting entry pressure of 1 barg. Table 2 shows measured non-wetting phase entry pressures of three porous water-oil membranes along with some reported properties. Polyacrylonitril (PAN) and Polytetrafluoroethylene (PTFE) were found suitable for water and oil, respectively, and were used in all experiments. To prevent potential damage from loose grains and stress on the membranes, slightly water-wet pre-filters (Vileda, Vileda Professional) were applied between the core and the membranes. The membranes were punched out to fit at least the diameter of the pressure ports and at most the diameter of the pre-filter. For all cores, the composite pressure taps were fixed to the core surface using epoxy glue (Quick-Epoxy, Biltema AS).

Table 2: Results of membrane non-wetting phase entry pressure (Pe) in a water-oil experiment.

| Material | Code | Manufacturer | Wetting | Pore Size | Pe (barg) |
|---|---|---|---|---|---|
| Polytetrafluoroethylene | PTFE | www.satorius.com | oil | 0.2μm | 2.40±0.05 |
| Polyacrylonitril | PAN | www.osmonics.com | water | 0.1 μm | 2.60±0.05 |
| Polysulfon | PS | www.nadir-filtration.com | water | 0.02-0.1μm | 14.65±0.05 |

Instead of a commercial rubber sleeve commonly used in coreflood experiments, epoxy glue was applied to seal the dry core including the pressure tap and end pieces. Different glues were tested, and the one finally used (Super-Epoxy, Biltema AS) was found to be liquid tight for more than 1 barg against an atmospheric confining pressure. The sealed cores were dried at 50$^{o}$C over night and before any injection of liquid, we pressurised the core by 2 bara of air, revealing and tightening possible leakages.

To stabilise clays, a 3.0 wt.% NaCl and 0.5 wt.% $CaCl_2$ brine solution was used and the dead oil phase was represented by Exxsol-D60. The laboratory condition viscosities of the fluids were measured to 1.04±0.01 cp and 1.33±0.02 cp for water and oil, respectively. The surface tension between these two fluids was previously measured in our laboratory to 30±2 mN/m.

The cores were evacuated, water was injected and using four pressure stages, the absolute permeability (k) was measured. Pulse-less pumps (Quizix QX-6000 and Quizix SP-5000, Quizix, Inc.), one for each fluid phase, were used to pump fluid through the core. Since our prototype resisted limited fluid pressure, drainage was done with increasing rates of 0.5, 1.0 and 2.0 ml/min and 0.2-2.0 ml/min in steps of 0.2 ml/min for cores P7 and P8, respectively. For P8, the rate was increased when no more water production and ΔP reduction could be observed. After the drainage, imbibition using a low rate of 0.5 and 0.1 ml/min for cores P7 and P8, respectively, was done. Because no equipment for measuring in-situ fluid distribution was available, saturations were measured by material balance at the outlet end of the core.

To assist the experiments, a 1D, 201 grid block, horizontal and homogeneous core simulation model was designed. The measured capillary pressure and relative permeability for core P8 were used in the model. A drainage process was simulated and from the production data, both traditional steady-state relative permeabilities and relative permeabilities based on phase pressure measurements were calculated.

## RESULTS

To improve the visualisation of the experimental results, experimental drainage pressure drops presented are reduced by interpolating the pressure linearly between the inlet and outlet pressure at the position of the pressure tap, x.

Figure 2 shows both measured ΔP and the water pressure (Pw) vs. time, measured through the PAN membrane during 100% waterflooding of core P4. A fast pressure response could be seen from the core through the membrane as the injection rate was changed. Figure 3 shows measured Pw at x/L = 0.34 in core P4 together with the interpolated ΔP vs. the position in the core for two different fractional flow of water (fw) injection rates of water and oil. It was observed that the water pressure was reduced relative to the interpolated pressure at the tap position as fw was reduced.

Figure 4 shows both the ΔP, and Pc measured at x/L = 0.40 vs. time during the drainage of core P7 using three increasing injection rates. While Pc was increasing for each rate, additional water was produced and the ΔP decreased. Figure 5 shows both measured ΔP and Pc measured through the differential pressure transducer for imbibition of core P7. The figure verifies that the capillary pressure drops to zero as the water front passes the pressure tap. The measured average Swi=0.43 and average residual oil saturation (Sor) was 0.17.

Figure 6 shows both the ΔP and Pc measured at x/L = 0.35 vs. time during the drainage of core P8 using 10 increasing injection rates. The pressure and production profiles were comparable to the results for core P7. Figure 7 shows both measured ΔP and Pc measured through the transducer during water injection of core P8. The measured residual saturations were Swi=0.40 and Sor=0.35, for drainage and imbibition, respectively.

Figure 8 shows measured drainage Pc vs. material balance Sw for core P8 during the dynamic flow process along with three sets of static drainage capillary pressure curves for Berea using the centrifuge method. The fluids and ambient conditions were equal in all the experiments. Because the dynamic data were collected during a flooding experiment, it was not possible to achieve the same Swi as for a static capillary pressure experiment. Figure 9 shows unsteady-state measured relative permeability for core P8. The large saturation gap lacking data, confirmed a considerable saturation shock in front of the spreading part of the saturation wave.

Figure 10 visualises the difference between traditionally calculated relative permeabilities and relative permeabilities retrieved from phase pressure and in situ saturation data during a simulated drainage steady-state experiment. The $\Delta P$ and the difference between inlet well pressure and phase pressure in grid block 71, counting from the injection block, were used for calculations for the two methods, respectively. Unlike the latter case, the traditionally calculated data became less accurate as the water saturation was decreased. The simulation study also showed that the end-effect was considerable at all rates, flawing the saturation calculations.

## DISCUSSION

The problems that were encountered when working with the setup should be mentioned. Firstly, the epoxy covering the core had a weak point around the core inlet, which in future work should be sealed off particularly well. Secondly, the membranes in general and especially the oil-wet Teflon membranes are made of very fragile material. For a successful application a smooth surface of the pressure transducer port is required; a sharp edge would easily damage the membrane.

The crucial part of this work was to achieve capillary contact from the pressure transducer over the membrane to the porous rock, along with preventing the non-wetting phase relative to the membrane to percolate through it. Interpreting Figures 4 through 7 shows that this challenge was overcome. In the case of the water-wet membrane, which was in contact with the low pressure port of the transducer, an oil leakage would result in a dramatic reduction in the measured capillary pressure, which is not observed during any of the drainage processes. Moreover, water is not likely to pass through the oil-wet membrane because Po is greater than Pw. Even if water should percolate through the Teflon membrane, it would still not alter the pressure reading because $Pc = 0$ inside the transducer port.

The increasing and eventually stable Pc after a rate changed during drainage (Figure 4 and 6) indicates that more water was produced from the pressure tap region. Moreover, at low rates the $\Delta P$ would flatten out at approximately the same time as the measured Pc. The observation supports our hypothesis that the time dilatation over the porous membrane is small. By using the compressibility of water and Darcy's law an expected pressure response delay of $< 1$ second is obtained. Comparing the results in Figure 4 to the results of Wunnik et al. [7] reveals that using a tiny pressure tap volume in the experiments probably will evade a pressure time delay problem.

This will allow for unsteady-state measurements if in-situ saturations can be provided.

Interestingly, as the injection rate was increased (Figure 6), the reduced ΔP exceeded the capillary pressure. As the saturation gradient in the core gradually decreases and approaches a horizontal linear profile when the injection rate is increased, the pressure gradient will eventually also become linear. It follows that the oil pressure at the tap position decreases relative to the injection pressure as Sor decreases.

Figure 7 reveals that the capillary pressure slightly increased before it dropped dramatically as the water front propagated beyond the transducer. This is believed to be caused by a locally increased oil pressure adjacent to the capillary interface between the fluids. Furthermore, fluctuations were observed as Pc decreases to 0. This observation can be explained by the nature of the unsteady-state process in a heterogeneous rock: Inside a cross-section of the core at the position of the pressure transducer, the water will enter at different locations at different times. Since Sw is increasing non-monotonically, the water pressure will vary until the water front has passed the area of the cross section. Behind the front, the capillary pressure is stable indicating a piston like regime of the experiment where no additional oil is mobile.

The difference in dynamic Pc compared to the static data shown in Figure 8 should be compared to the results of Kaladijan [10]. His results for limestone and Berea showed increasing difference in capillary pressure for increasing difference in injection rates, which is in good agreement with our observations. He also found that dynamic capillary pressure is very sensitive to the flow rate. However, the capillary number for our experiments were about 10 times greater than reported in his work, imposing a more viscous dominated flow, which complicates the comparison of the results. Moreover, even though our cores were longer than a typical core plug, the end-effect could possibly be responsible for an overestimation of Sw by using average saturations. However, a decreasing end-effect with increasing Pc (increasing rate) is expected, while in Figure 8 the difference in Sw seems constant for all Pc-values. Hence, it is doubtful that the end-effect alone explains the observed shift in the curve.

If equilibrium capillary pressure data measured in a separate experiment (e.g. by the porous plate method) is available, the error shown in Figure 10 can conventionally be reduced by history matching the experimental production data. As shown in Figure 8, these data might be different from conventional Pc data when measured during a dynamic production process. To find the root cause for the observed difference, however, further investigation is required.

## CONCLUSIONS

The work described in this paper confirms successfully measured water and oil phase pressures inside a porous rock. The method can be used for both imbibition and drainage flowing processes with only modest modifications of a conventional relative permeability apparatus.

Drainage dynamic capillary pressure data have been estimated. These data are considerably greater in magnitude compared to static data. However, due to the relatively low capillary pressures reached during a flooding process, it is not known if the Pc-curves for the static and dynamic processes merge to the same asymptote towards the irreducible water saturation. Also, it is not known if the cores are sufficiently long to neglect the impact of the end-effect, possibly contributing to the difference in dynamic and static Pc-data.

The experimental setup used is well designed for steady-state experiments. Additionally, the time delay over the membrane is optimistically small, and using realistic reservoir rates will probably support an application to an unsteady-state coreflood.

To invert relative permeabilities using in-situ data, measurements of the saturation profile inside the core is required along with the in-situ Pc-values. The improvement from a traditional procedure, where no Pc-data are applied, is easily shown by simulation.

## ACKNOWLEDGEMENTS

The authors would like to thank Hydro ASA for providing founds for this work. Also, discussions with Erik Lindeberg and Idar Akervoll at Sintef Petroleum Research, Jann-Rune Ursin, Svein Skjæveland the University of Stavanger and Fred Bratteli at Rogaland Forskning have been of great importance to the authors.

## NOMENCLATURE

x = Distance to pressure tap, L = Length of core, Pc = Capillary pressure at tap position, $\Delta P$ = Pressure drop over the core, Pw = Water pressure at tap position, Swi = Irreducible water saturation, fw = fractional flow of water, krw = Relative permeability to water, kro = Relative permeability to oil, Sor = Residual oil saturation.

## REFERENCES

1. Honarpour, M.M., Koederitz, L.F., “Relative Permeability of Petroleum Reservoirs,” CRC Press Inc., Boca Raton, 1987.
2. Kokkedee, J.A., Boom, W., Frens, A.M., Maas, J.G., “Improved Special Core Analysis: Scope for a reduced residual oil saturation,” SCA-9601 in Proceedings of the 1996 International Symposium of the SCA, Montpellier, France, 8-10 September 1996.
3. Hassler, G.L., Brunner, E., “Measurement of Capillary Pressure in Small Core Samples,” Trans. AIME (1945) **160**.
4. Schembre, J.M., Kovscek, A.R., “A Technique for Measuring Two-Phase Relative Permeability in Porous Media via X-ray CT Measurements,” J. Petr. Sci. and Eng., (2003) **39**,159-174.
5. Zolotukhin, A.B., Ursin, J-R., “Introduction to Petroleum Reservior Engineering,” Høyskoleforlaget, Norwegian Academic Press, 2000.
6. Richardson, J.G., Kerver, J.K., Hafford, J.A., Osoba, J.S., “Laboratory Determination of Relative Permeability,” Trans. AIME, (1952), **195**, 187-96.

7. Wunnik, J.N.M., Oeday, S., Masalmeh, S., "Capillary Pressure for SCAL Application," SCA-9908 in Proceedings of the 1999 International Symposium of the SCA, Golden, Colorado, 1-4 August 1999.
8. Amyx, J.W., Bass, K.M., Whiting, R.L., "Petroleum Reservoir Engineering Physical Properties," McGraw-Hill, New York, 1960.
9. Honarpour, M.M., Huand, D.D., Rafi Al-Hussainy, "Simultaneous Measurement of Relative Permeability and Capillary Pressure, and Electrical Resistivity with Microwave System for Saturation Monitoring," paper SPE 30540 presented at the SPE Annual Technical Conference and Exhibition, Dallas, TX, 22-25 October 1995.
10. Kaladijan, F.J-M., "Dynamic Capillary Pressure Curve for Water/Oil Displacement in Porous Media: Theory vs. Experiment," paper SPE 24813 presented at the 67th Annual Technical Conference and Exhibition of SPE, Washington, DC, 4-7 October 1992.
11. Lenormand, R., Eisenzimmer, A., Delaplace, Ph., "Improvements in the Semidynamic Method for Capillary Pressure Measurements," SCA-9531 in Proceedings of the 1995 International Symposium of the SCA, San Francisco, CA, 12-14 September 1995.
12. Ursin, J.R., Mannes, T., "Fluid Phase Pressure Measurements," Tech. Report. Stavanger College. 1996.
13. Helset, H.M., Nordtvedt, J.E., Skjæveland, S.M., Virnovsky, G.A., "Three Phase Relative Permeabilities with full Account for capillary pressure," SPE paper 36684 presented at the SPE Annual Technical Conference and Exhibition, Denver Colorado, 6-9 October 1996.
14. Virnovsky, G.A., Skjæveland, S.M., "Steady-State Relative Permeability Measurements Corrected for Capillary Effects," paper SPE 30541 presented at the SPE Annual Technical Conference and Exhibition in Dallas, Texas, October 1995.

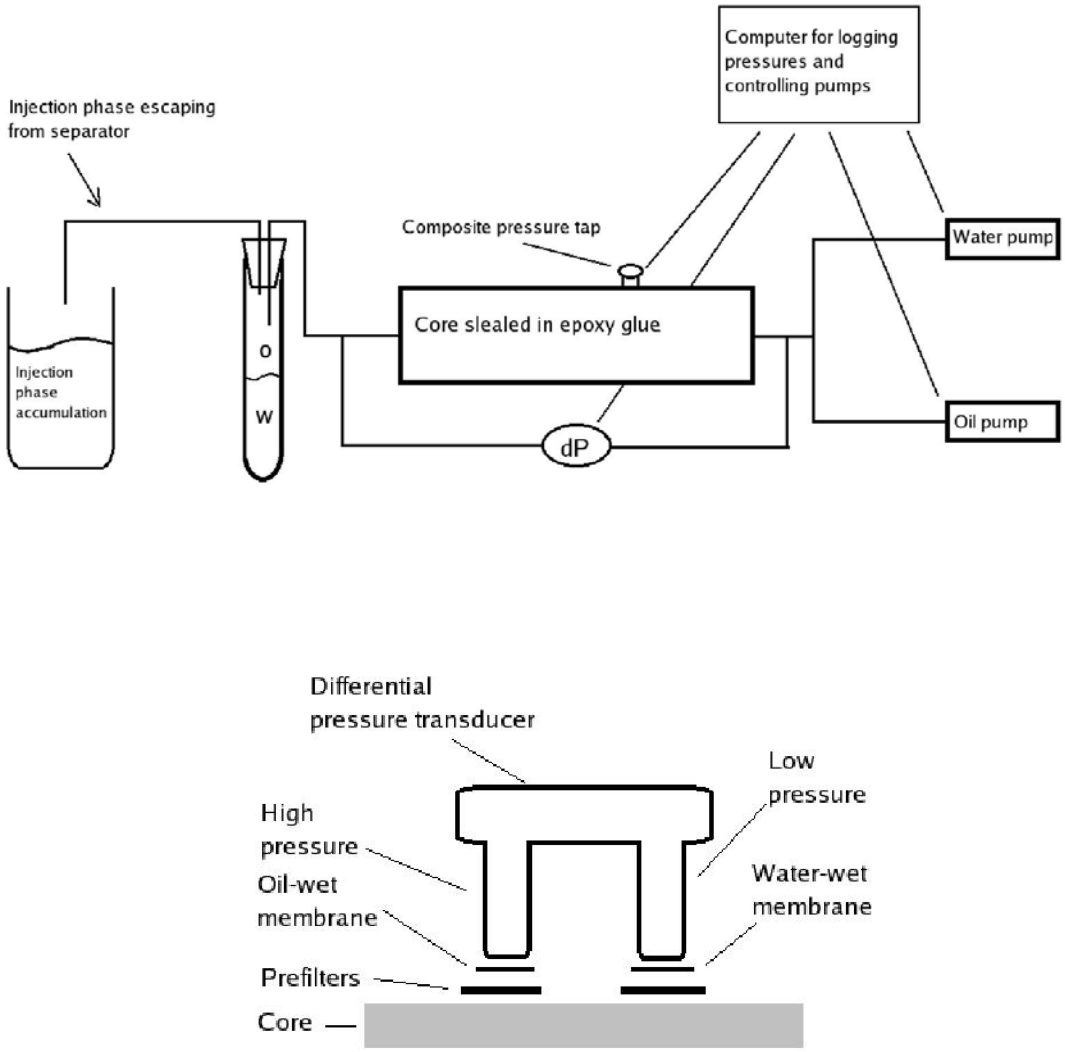


**Figure 1: Top: Sketch of the overall experimental setup. Bottom: Components of the pressure tap arrangement. Individual water and oil pressures are recorded in the low and high pressure pins, respectively.**

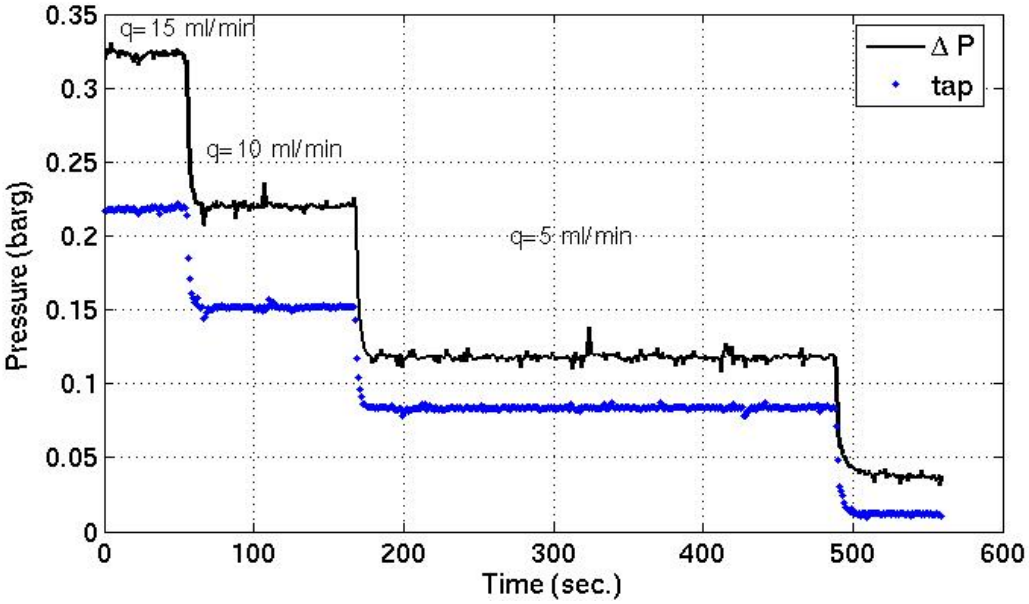


**Figure 2: Pressure response through the porous membrane during absolute water permeability measurement. Because of the small transducer volume (0.01 ml), changes in the core pressure was immediately recorded.**

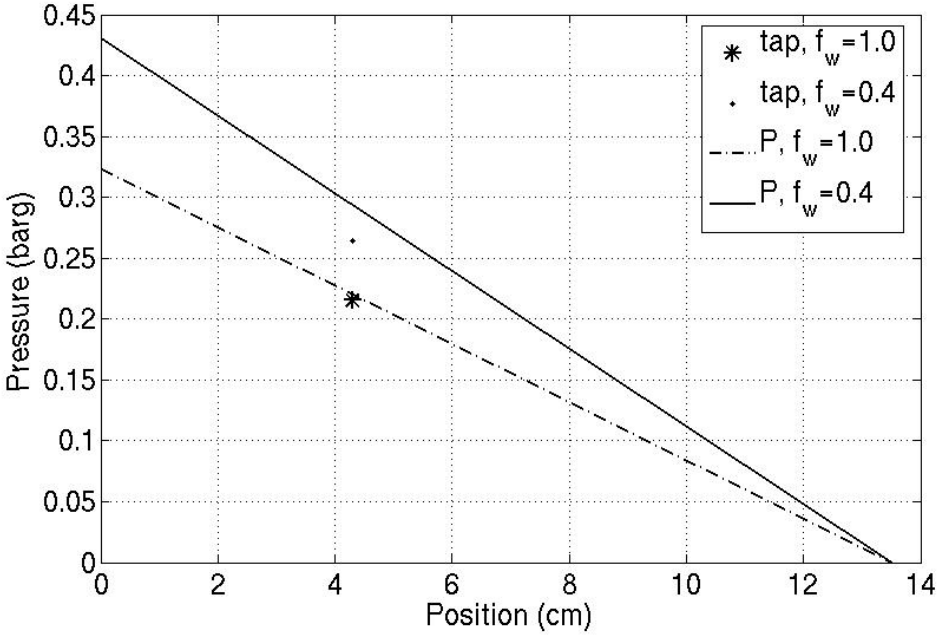


**Figure 3: Effect of fractional flow rate of oil and water on measured water pressure (*) with pressure drop (line) for a Bentheimer core. We measured water phase pressure at x/L=0.32.**

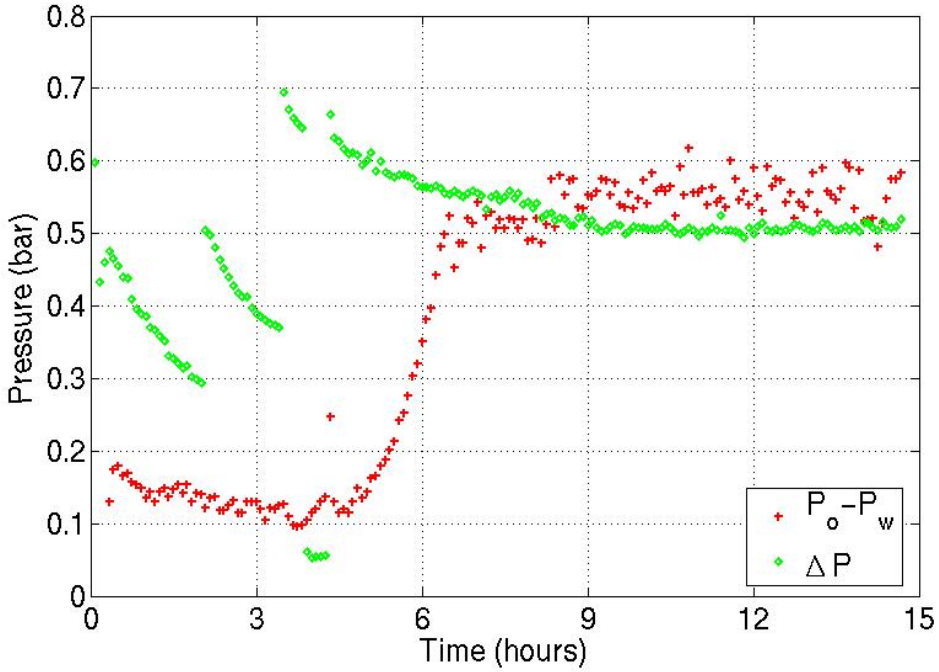


**Figure 4: Measured ΔP and Pc at x/L=0.35 vs. time during the drainage of P7.**

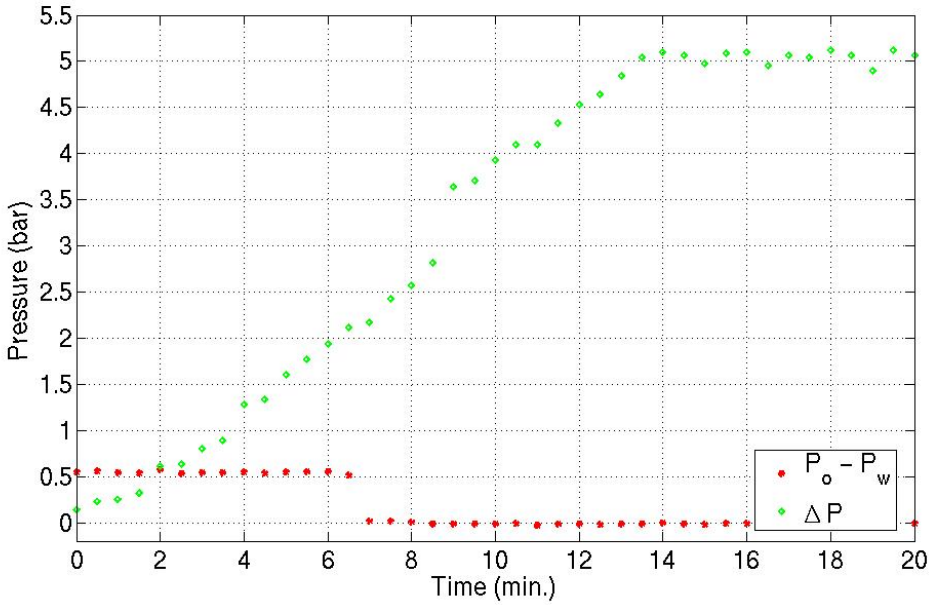


**Figure 5: Measured ΔP and Pc at x/L=0.40 vs. time during water injection of P7. The capillary pressure reduces to zero as the water front passes the point of the pressure transducer.**

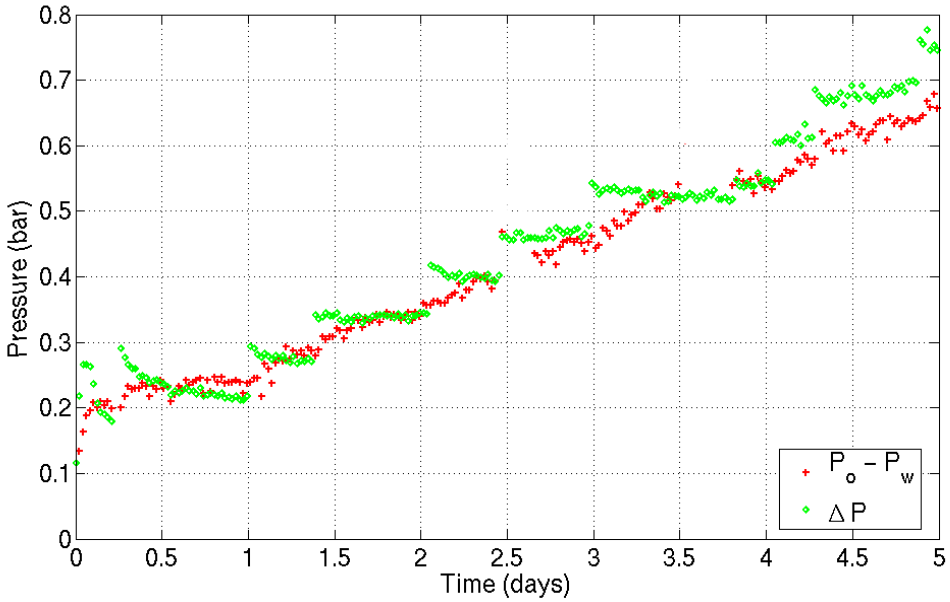


**Figure 6: ΔP over the core and Pc at x/L=0.35 vs. time during drainage of P8. As the rate was increased, additional water was produced, the ΔP declined while Pc was observed to increase.**

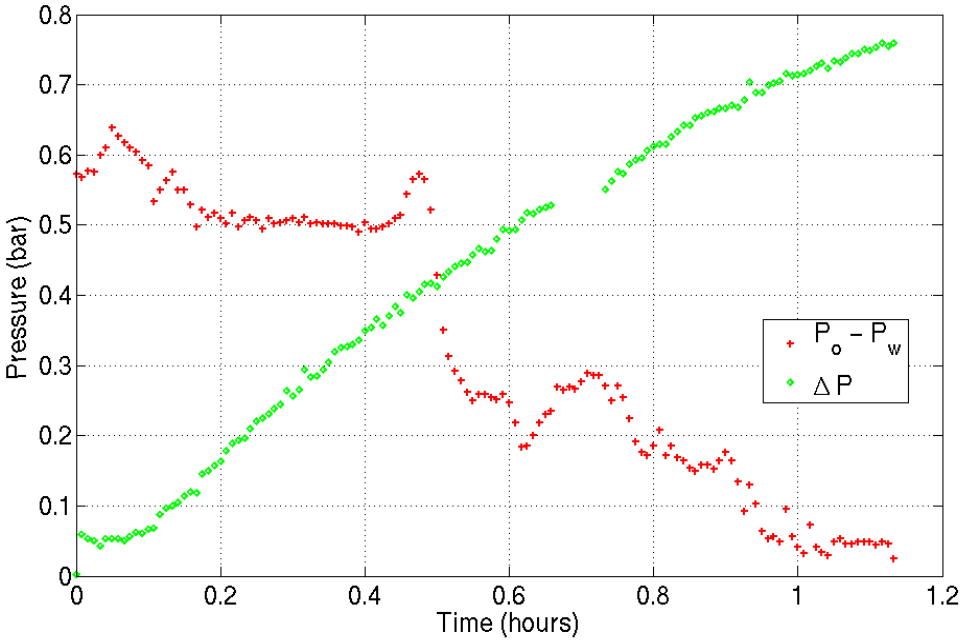


**Figure 7: Measured ΔP and Pc at x/L=0.35 vs. time during water injection of P8. Note that slight increase in capillary pressure before the water front passes the transducer.**

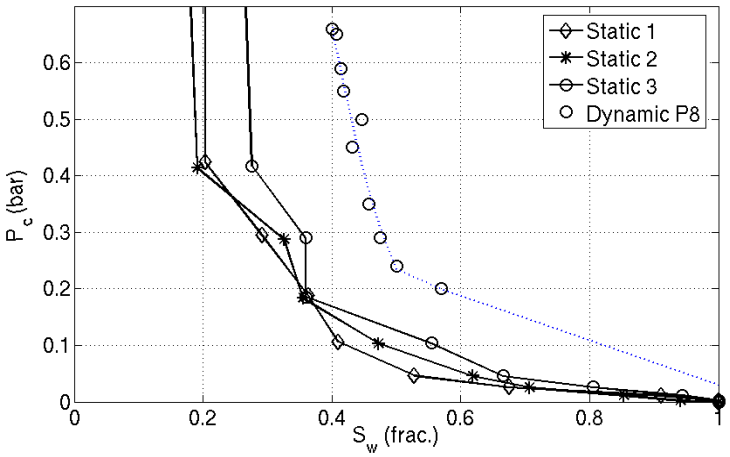


**Figure 8: Dynamic capillary pressure for P8 during drainage together with previously measured static capillary pressure curves.**

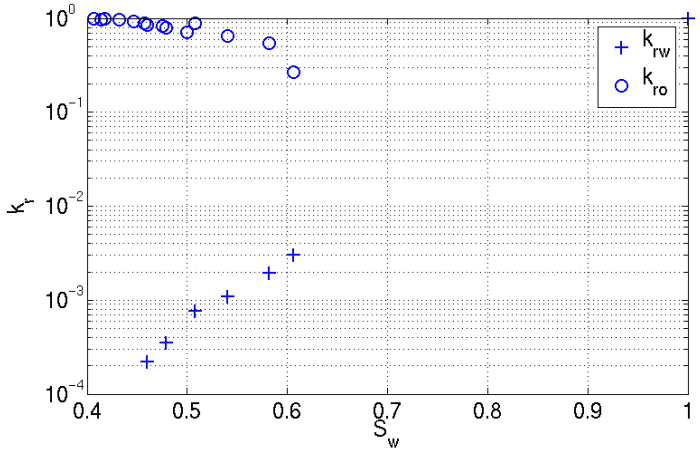


**Figure 9: Measured drainage relative permeability for P8.**

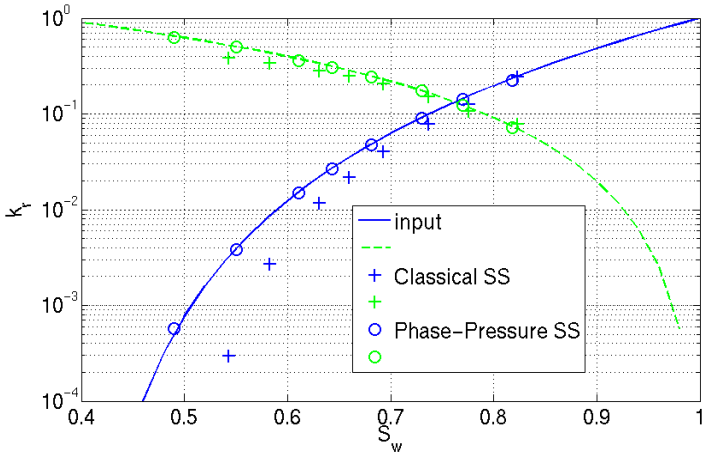


**Figure 10: Drainage relative permeability measured for simulated flow data using both traditional steady-state data and phase pressure data with in situ saturations.**